Blind Spot Eliminator: Collaborative Point Cloud Perception in Cellular-V2X Networks

Ziyue Chen, Guiyang Luo, Congzhang Shao, Quan Yuan and Jinglin Li
State Key Laboratory of Networking and Switching Technology
Beijing University of Posts and Telecommunications
Beijing, China
{bupt_czy, luoguiyang, shaocongzhang, yuanquan, jlli}@bupt.edu.cn

***Abstract*—Multi-agent collaborative perception depends on sharing sensory information to improve perception accuracy and robustness, as well as to extend coverage. However, most collaborative perception methods ignore the limitations of communication networks, such as limited bandwidth and the possibility of wireless conflicts. To fill this gap, this paper proposes BlindSpotEliminator, a conflict-free scheduler over the cellular-V2X networks for supporting practical collaborative point cloud perception to eliminate blind spots. BlindSpotEliminator first identifies the blind spots for each vehicle, then lists the corresponding conflict relationships based on the distribution of the blind spots and communication conflicts, and finally designs an optimized point cloud data transmission strategy to eliminate the blind spots of each vehicle. Extensive experiments show that compared with greedy algorithm and random methods, BlindSpotEliminator achieves better efficiency, i.e., transmitting 20% more point cloud data.**

***Index Terms*—collaborative perception, point cloud data transmission, optimization strategy, Cellular V2X**

I. Introduction

As a crucial aspect of autonomous driving, perception is responsible for obtaining and analyzing environmental information to enable the vehicle to detect other traffic participants. Equipped with on-board sensors such as LiDAR, cameras, and other equipment, autonomous driving vehicles achieve a comprehensive and robust real-time perception of their surrounding traffic environment, e.g., FADNet [1], Pointformer [2], Pixor [3], TDRF [4]. Traditionally, autonomous driving perception technology has been centered around single vehicle intelligence. However, with industry development, single vehicle perception technology has encountered bottlenecks, such as the inability of perceiving blocked or distant objects. These limitations render it challenging for a single vehicle to effectively perceive the surrounding traffic environment, potentially leading to traffic accidents. To overcome these challenges, collaborative perception [5], e.g. Who2com [6], Federated Vehicular Transformers [7], FSCOD [8], takes advantage of network communication capabilities. By leveraging sensory data from multiple vehicles, this approach significantly enhances the perception range of each vehicle and reduces uncertainty in the perception process. By analyzing collective data, vehicles can better understand their surroundings and make more informed decisions [9].

Nevertheless, most collaborative perception methods ignore the limitations of communication networks. Vehicles generate vast amounts of data during driving, such as point cloud data, pictures, and depth of field pictures, with data redundancy between different vehicles. Although paper [10] considers the limitations of communication networks, it focuses more on how to address data corruption caused by the attenuation of wireless networks. We consider using Cellular V2X communication network to address this issue. Cellular V2X [11], or "Cellular Vehicle to Everything" communication, is an emerging technology that utilizes and enhances existing LTE functionality and network elements to facilitate V2X message exchange. Specifically, in addition to traditional uplink/downlink connections, LTE V2X enables device-to-device (D2D) mode through the LTE PC5 interface based on the 12th Neighbor Discovery Service. This interface provides D2D communication called sidelink (SL), which reuses parts of the uplink frame and supports allocation mode 3. In mode 3, the transmission on the sidelink is authorized by the network, making it a centralized approach. The standard provides freedom for SL scheduling in mode 3, which manages and allocates sidelink resources under cellular network coverage. This paper utilizes this advantage to develop an efficient collision-free method for reserved resource allocation mode 3 in cellular V2X.

While Cellular-V2X communication networks offer high bandwidth and low latency, they may face limitations in transmitting all the data associated with complex traffic scenarios. This becomes particularly evident when multiple vehicles attempt to transmit data simultaneously, leading to interference and decreased data transfer rates. Hence, designing an efficient data scheduling algorithm specifically for collaborative perception scenarios is essential to transmit as much meaningful data as possible while avoiding communication collisions. Designing an efficient data scheduling algorithm for collaborative perception using Cellular-V2X communication network meets the following challenges:

- What data format to choose for transmission? The choice of data format for transmission would depend on factors such as the nature of the data, the bandwidth available, and the desired level of accuracy. For example, point cloud data may provide a more detailed representation of the environment [12], but may require more bandwidth than images. Therefore, a trade-off needs to be made

between the level of detail required and the available bandwidth.
- What data should be transmitted by each vehicle? Due to the possibility that different vehicles may observe redundant point cloud data, transmitting all of this data can result in a wastage of communication resources. Therefore, it is essential to develop a scheme that can choose which area of data to transmit to other vehicles for each vehicle. This can involve designing algorithms or protocols that consider factors such as the relevance and importance of the data and the available communication bandwidth.
- Considering the relationship of wireless conflicts, how to schedule these data to be transmitted in the communication network and effectively avoid communication collisions? To schedule the data transmission, it is necessary to consider the communication conflicts that may arise due to multiple vehicles trying to transmit data simultaneously. To avoid collisions, a scheduling algorithm needs to be designed to take into account the availability of communication channels, the priority of the data, and the distance between the vehicles.

This paper proposes an innovative algorithm called BlindSpotEliminator for conflict-free communication resource allocation. BlindSpotEliminator is specifically designed for the framework defined by the cellular V2X standard. We choose to transmit raw point cloud data as the selected data format to ensure efficient data transmission. Additionally, BlindSpotEliminator defines the blind spot of each vehicle, which helps identify the areas that require special attention during communication. Then BlindSpotEliminator defines the mapping relationship between communication resources and links, as well as a conflict graph describing the entire communication conflict topology. Furthermore, due to the scarcity of V2X resources, resource reuse opportunities should be utilized in cellular V2X. In other words, BlindSpotEliminator must consider the reuse of the same communication resources by interference-free links. Based on this, BlindSpotEliminator designed an optimization strategy for complex traffic scenes to transmit as much valuable point cloud data as possible and eliminate blind spots while considering resource reuse to maximize resource utilization efficiency.

Furthermore, we evaluate the effectiveness of BlindSpotEliminator in complex traffic scenarios using the Carla simulator. We use the simulator data to evaluate BlindSpotEliminator and design corresponding metric for collaborative perception. We also include greedy and random allocation algorithms as baselines for comparison. Our experimental results show that BlindSpotEliminator not only enhances the perception range but also achieve higher communication resource utilization rate. Furthermore, we evaluate the effectiveness of BlindSpotEliminator in complex traffic scenarios using the Carla simulator. We use the simulator data to evaluate BlindSpotEliminator and design corresponding metrics for collaborative perception. We also include greedy and random allocation algorithms as baselines for comparison. Our experimental results show that BlindSpotEliminator enhances the perception range and achieves a higher communication resource utilization rate.

II. Releated Works

Communication scheduling algorithms play a crucial role in V2X communication and have garnered significant attention from academia and industry in recent years. These algorithms are responsible for efficiently managing communication resources. Currently, there are three main types of scheduling algorithms for vehicular communication:

1) Multi-agent reinforcement learning: In [13], a deep reinforcement learning-based SPS (RL-SPS) algorithm is proposed using multi-agent learning to help agents select suitable wireless resources and reduce packet collisions. In CommNet [14], an attention module is placed to measure the importance of other agents' data, which decides the communication target. In the collaborative perception scenario, When2com [15] uses self-attention and cross-attention to determine whom to communicate with. Software-defined networking (SDN) [16] utilizes centralized intelligence to manage and allocate communication resources. Based on SDN, [17] models point cloud resource scheduling as a partially observable Markov decision process (POMDP) and uses value iteration to optimize network, caching, and computing jointly. Due to the complex coupling of point cloud resources, it is challenging for the central controller to know in advance how its actions affect system performance. Thus, [18] proposes a deep reinforcement learning (DRL)-based resource orchestration method that enables the central controller to learn effective policies through trial and error search. SMORL [19] integrates three key components, namely a computationally efficient model-based trajectory optimizer to reduce cost. [20] leverages monocular camera data to assist in the perception of LiDAR data.
2) Modeling optimization: In [21], the original scene topology graph is constructed as a three-level subtree, where the first-level child nodes communicate with the network management node, and the second-level child nodes are multiple non-conflicting nodes that complete communication by invoking the parent node's communication ability. [22] proposes a directed conflict graph and undirected coexistence graph-based method for calculating the communication order of vehicles and respectively employs depth-first search and minimum clique cover algorithm to compute the optimal order. Based on SDN, [23] converts the current traffic communication relationship into a conflict graph and transforms the problem into finding the maximum independent set problem to minimize the overall network communication delay. [24] transforms the original problem into the traveling salesman problem and attempts to find the minimum number of communication channels to meet as many

communication requirements as possible. In [25], the communication topology of the highway traffic scenario is established as an inherent ordered tree structure. The delay perception in LTE frames is used as the scheduling metric, and the problem is transformed into a shortest path problem to minimize overall communication delay. In [26], the Lyapunov optimization theory is integrated into the long-term dynamic resource allocation framework.

3) Integer programming: The central idea of this type of method is to transform the resource scheduling problem into an optimization problem based on the constraints and requirements of the current scenario. In [27], the overall transmission plan is transformed into a maximum-minimum optimization problem based on the conflict graph to reduce the required communication resources and transmission delay. [28] transforms the problem of finding the minimum number of channels into a binary optimization problem, intending to minimize the number of communication channels required to meet the vehicle-to-everything (V2X) communication scenario. [29] finds a set of non-conflicting scheduling plans in a multicast environment and transforms the problem of minimizing the end-to-end delay into an integer programming problem. [30] proposes a joint autonomous resource selection and scheduling resource allocation method to maximize the total information value of all users and achieve the highest overall resource utilization. Paper [31] includes a multi-access edge computing system to address the issue of long computation time in integer programming.

In addition to the three methods mentioned earlier, there are other approaches. For example, in [32], a single Dynamic Bayesian Network (DBN) is used to jointly model the topology to avoid collisions. Paper [33] employs Model predictive control (MPC) using randomized optimization to address various communication control problems. The paper [35] proposes a Radar-Communication (R-Comm) algorithm which enables connected vehicles to use a fraction of radar resources for vehicular communication based on the traffic density. The paper [34] uses trajectory analysis of surrounding vehicles to evaluate risk and prevent communication collisions.

Although existing methods can achieve communication resource allocation, some issues still need to be addressed. First, the data may have redundancy, which requires avoiding transmitting the same data from different vehicles. Second, the data to be transmitted needs to be clearly defined. In real-world traffic scenarios, it is necessary to transmit blind spot data for autonomous vehicles. Finally, most of these methods assume that communication resources are not limited, but communication resources are always limited in real traffic scenarios. To address the mentioned issues, this paper first defines blind spots from the perspective of point cloud data to clarify the data that needs to be transmitted. Then, this paper designs a set of optimized transmission strategies, which considers reducing data redundancy, communication resource reuse, and communication conflict avoidance to minimize blind spots.

III. Preliminaries

A. LTE Frame Structure

Each LTE frame is divided into time slots in the time domain and resource blocks (RB) in the frequency domain, with two consecutive time slots forming a subframe. We define a transmission block (TB) as the smallest unit of resources that can be allocated to the V2X sidelink in a 20MHz channel. Each TB is a block of n contiguous RBs in a subframe, and thus, the two dimensions of the resource space are the channel and TB. For proper transmission, each data packet must be associated with a control information (CI) field containing essential control data such as the time slot and RB where the packet begins, its length, and source and destination node addresses. The CI occupies a fixed number of contiguous RBs in a subframe and may be sent adjacent to the data packet or in another designated portion. We define packet scheduling as contiguous if all requests are assigned to contiguous TBs. Due to the V2X standard configuration, such subsequent assignments result in minimum CI. This is in contrast to non-contiguous scheduling, which allows splitting the data packet into separate TBs and results in CI overhead. In this paper, we limit the scheduler to non-contiguity. Although non-contiguity may increase CI overhead, contiguous allocation increases overall computational complexity, making the system unable to meet real-time requirements.

B. Point Cloud Data and Blind Spots

This paper focuses on the perception task of LiDAR-based object detection, as the unified 3D space naturally allows for the aggregation of multiple LiDAR scans. Each LiDAR N_i can periodically generate point clouds $P_i = \{p_i^1, p_i^2, \dots\}$, where $p_i^j = [x, y, z, r]$, and (x, y, z) is the 3D coordinates and r is the reflectance intensity.

Inspired by object detection algorithms that significantly improve detection accuracy using point cloud data, e.g., Voxnet [36], Voxelnet [37], PointPillars [38], RangeSeg [39], which partitions the entire point cloud data into multiple equally sized cubic grids. We adopt a similar approach to model the traffic scene and divide it into multiple equally sized cubic grids, representing all grid numbers in the current scene. Each grid o contains a certain number of points and can be represented as (x, y, P_i^o), where x and y denote the location of the grid, and P_i^o is the set of points belonging to grid o. At the same time, we limit the number of points in each grid based on the lessons learned from detection algorithms, which is represented as P_{max}. We set P_{max} in advance, and for grids with data exceeding P_{max}, We randomly sample P_{max} points. We consider zero padding for the grids with a point count lower than P_{max} to make the point cloud count consistent for all grids, which is to facilitate the subsequent object detection algorithm.

After voxelizing the entire region, it is necessary to determine which grids are blind spots. Suppose there are two

vehicles, vehicle A and vehicle B. If vehicle B can observe the point cloud data of grid o and the number of point cloud data observed by B exceeds or is equal to P_{max}. However, vehicle A cannot observe any points, and then we add grid o to the list L_A^B(symbol L_A^B represents the list of grids that can be observed by vehicle B but not by vehicle A). For vehicle A, the continuous area composed of several grids in L_A^B is a blind spot for vehicle A. Since a vehicle may exchange data with multiple vehicles, a blind spot in the perspective of one vehicle may be observed by different vehicles simultaneously. We use the set $B_i = \left\{b_i^{0,1}, b_i^{0,2}, \ldots, b_i^{j,k}\right\}$ to represent the blind spot of vehicle i, where the element $b_i^{j,k} = \{o_1, o_2, \ldots, o_j\}$ represents the set of grids observed by vehicle j about the blind spot k.

IV. System Model

A. Collaborative Perception Process

Our scenario involves an edge computing node responsible for coordinating point cloud data communication among all intelligent vehicles at a crowded urban intersection, as shown in the figure. The intelligent vehicles are all equipped with LiDAR and are willing to share their point cloud data with other vehicles to enhance overall collaborative perception. The entire collaborative perception service process can be divided into the following parts:

- Upload phase: In each time slot, all collaborative perception participants (i.e., intelligent vehicles that are willing and capable of participating in collaborative perception) first upload the distribution of their observed point cloud data to the edge computing node. Because only the point cloud data distribution needs to be uploaded rather than the raw data, the overall data volume is significantly reduced, and the transmission delay is reduced to milliseconds.
- Computing phase: After receiving the data distribution from all vehicles, the edge computing node uses an optimization strategy to command pairwise data transmission among intelligent vehicles, reducing the number of blind spots observed by vehicles while ensuring that communication links do not collide.
- Transmission phase: The edge computing node delivers the corresponding point cloud data transmission scheme to the corresponding vehicles, which then communicate with other vehicles according to the scheme.
- Object detection phase: The vehicles combine the received point cloud data from other vehicles with their own observed point cloud data, call the object detection algorithm to process the complete data, and obtain more accurate and robust object detection results.

In order to ensure that the point cloud data from different vehicles can be merged together, it is necessary for all the collaborative perception participants to have strictly uniform grid sizes and distribution patterns. Moreover, the coordinate systems of the point cloud data observed by different vehicles may not be consistent, so an affine transformation is needed to align the coordinate systems of the point cloud data from all the intelligent vehicles. For simplicity, the set of grids is denoted as O. Each participant i can observe a subset of pillars $O_i \subseteq O$, and the set of points in pillar $o \in O_i$ is P_i^o. Participants cooperatively disseminate points to each other, for broadening the perception range and enhancing detection accuracy and robustness.

B. System Model

Based on the scenario described, the transmission phase is divided into a set of time slots $\mathbf{T} = \{1, 2, \ldots, T\}$, which contains T time slots. The length of each time slot is consistent with the fixed size of an LTE frame time slot for Cellular V2X communication. Therefore, the amount of point cloud data transmitted by a single resource block in a single time slice is fixed, and N_s represents the number of points that a single resource block can carry in a time slot. In the original LTE frame, assigning communication resources requires determining the communication frequency and the corresponding resource block number. To simplify the calculation, we unify the resource blocks and obtain a set $\mathbf{R} = \{1, 2, \ldots, r\}$, where the total number of resource blocks is equal to r. To ensure communication quality, we limit communication to only intelligent vehicles within a distance l_e. An intelligent vehicle's effective communication range may contain multiple intelligent vehicles. We obtain a set of communication links $\mathbf{C} = \{c_1, c_2, \ldots, c_m\}$. For any element c_j in the set, it describes a communication link from one vehicle to another vehicle. We use set $\mathbf{d} = \{d_1, d_2, \ldots, d_m\}$ to represent each link's required number of resource blocks. For any element d_j belonging to set $\mathbf{d}$, it should be a natural number.

For any given time slot t, the edge computing node directs the vehicles to transmit as much valuable point cloud data as possible between them, based on the current distribution of point cloud data of the intelligent vehicles in the scene and communication resource constraints. This process is determined by a set of optimization strategies designed in this paper. The optimization calculation times is equal to the number of time slots in the transmission phase. In a single optimization calculation, the following constraints exist:

1) Demand calculation: Before calculation, we need to calculate the demand for resource blocks based on the blind spots of each vehicle. For a link from vehicle i to vehicle j, the communication resource demand should be the total amount of point cloud data from all the blind spots that vehicle j cannot observe but vehicle i can observe. Therefore, we use the set $\mathbf{D} = \{D_1, D_2, \ldots, D_m\}$ to represent the point cloud data demand for a communication link.

$$D_q = P_{max} * \sum_{\forall b_i^{j,k} \in B_i} |b_i^{j,k}|, c_q = i \rightarrow j \tag{1}$$

$$d_q = \lfloor \frac{D_q}{N_s} \rfloor, 1 \leq q \leq m \tag{2}$$

2) Resource block allocation: We use the symbol $x_{i,j}$ to indicate that resource block i is allocated to link j, and

the value of $x_{i,j}$ is either 0 or 1. 0 represents that resource block i is allocated to link j, and vice versa represents unallocated.

$$0 \leq x_{i,j} \leq 1, i \in \mathbf{R}, c_j \in \mathbf{C} \tag{3}$$

3) Resource demand constraint: We use the symbol y_j to represent the required number of resource blocks for link j. The number of resource blocks allocated to link j can be at most its demand. We use a set $\mathbf{Z} = \{z_1, z_2, \ldots, z_m\}$ to represent whether a link is activated, and the range of any element in the set $\mathbf{Z}$ is 0 or 1. For z_j $\mathbf{Z}$, its value equal to 1 represents that link j is activated; on the contrary, it means that j is not activated.

$$y_j = \sum_{\forall i \in \mathbf{R}} x_{i,j}, c_j \in \mathbf{C} \tag{4}$$

$$y_j \leq d_j, c_j \in \mathbf{C} \tag{5}$$

$$z_j = sign(y_j), c_j \in \mathbf{C} \tag{6}$$

where sign() is Signum function.

4) Conflict avoidance: To avoid communication conflicts in the Cellular V2X network, we must consider two conflicts that may occur during communication. The first type of conflict is that a vehicle cannot send and receive data simultaneously within a time slot. The second type of conflict, known as distance-based conflict, occurs when multiple data senders exist within the conflict range of the data receiver. In this case, each data sender must use a different resource block to avoid conflicts. The distance parameter l_c defines the conflict range.
To better represent the conflict relationships, this paper introduces a conflict graph $\mathbf{G}_c = (\mathbf{V}, \varepsilon^f, \varepsilon^s)$ to depict the two types of conflicts mentioned earlier. The node set of the conflict graph $\mathbf{V} = \{1, 2, \ldots, m\}$ represents communication links, where the length of $\mathbf{V}$ is the same as the length of $\mathbf{C}$, while the edge set ε^f indicate whether there is a first conflict relationship between two links and edge set ε^s indicate the second conflict relationship. We denote the conflict relationship in terms of the first conflict of the second conflict as $\mathbf{G}_c^f(i,j)$ and $\mathbf{G}_c^s(i,j)$, respectively, where it is true if link i is a conflict with link j. In particular, the value of $\mathbf{G}_c^f(i,i)$ and $\mathbf{G}_c^s(j,j)$ are always false. Thus, we obtain the new constraint expressions:

$$z_j \wedge z_k = 0, if \mathbf{G}_c^f(j,k) = 1, \forall j \in \mathbf{V}, \forall k \in \mathbf{V} \tag{7}$$

$$x_{i,j} \wedge x_{i,k} = 0, if \mathbf{G}_c^s(j,k) = 1, \forall i \in \mathbf{R}, \forall j,k \in \mathbf{V} \tag{8}$$

where $\wedge$ stands for AND symbol.

5) Optimization object: given that redundant point cloud data has been removed during demand calculation and that the allocation of resource blocks to each communication link has been ensured to avoid conflicts, the optimization objective is to maximize the total number of resource blocks allocated to all communication links. Symbolically, we can express this objective as follows:

$$\max \sum_{1 \leq i \leq m} d_i \tag{9}$$

$$\text{s.t.} (1), (2), (3), (4), (5), (6), (7), (8)$$

V. SIMULATIONS

In this section, we compare BlindSpotEliminator with greedy and random contention algorithms. Section V-A presents the two comparison methods' specific details and evaluation metrics. Section V-B provides the Quantitative Evaluation of the three methods. Section V-C explains the superiority of BlindSpotEliminator by implementing specific details.

Fig. 1: The bird's-eye view photograph.

A. Comparison Algorithm and Metric

There are two methods used for comparison. The first method is the greedy algorithm, which sorts all possible transmission links in descending order based on their valuable point cloud data size. It then selects the link with the highest data size and assigns communication resources to it, provided it does not conflict with previously allocated links. If there is a conflict, it is skipped, and the process continues until all links have been traversed. The second method is a randomized algorithm, which randomly sorts all possible transmission links and traverses them from the beginning. Communication resources are assigned if a link does not conflict with already allocated links. Otherwise, it is skipped.

To effectively evaluate the scheduling performance of different scheduling algorithms, we use the total number of transmitted points to assess the scheduling effectiveness. This metric allows us to measure the extent to which the scheduling algorithms address blind spots, ensuring that each transmitted point belongs to an area the receiver cannot perceive. Considering the half-duplex constraint, where each vehicle can only exchange data with another vehicle in a time slot, we can ensure that each transmission avoids redundant data. Before each transmission, blind spots are recalculated to prevent redundancy. Given that every transmitted point holds significance, we utilize the total number of transmitted points as the comprehensive evaluation metric.

B. Quantitative Evaluation

To illustrate the transmission efficiency of the BlindSpotEliminator in a complex traffic scenario, we designed a complex

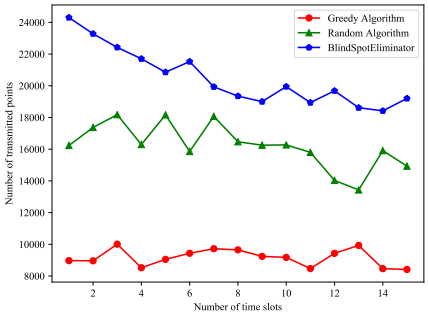

(a) Line graph of the number of transmitted points as time slot quantity varies.

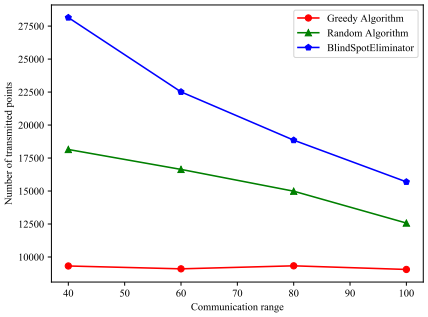

(b) Line graph of number of transmitted points as V2X communication range varies.

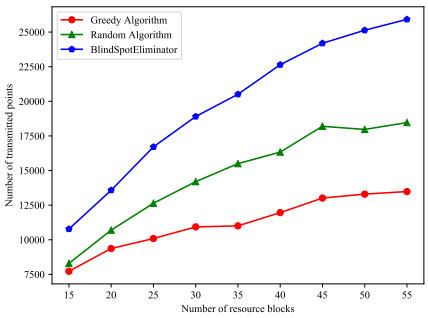

(c) Line graph of number of transmission points as resource block quantity varies.

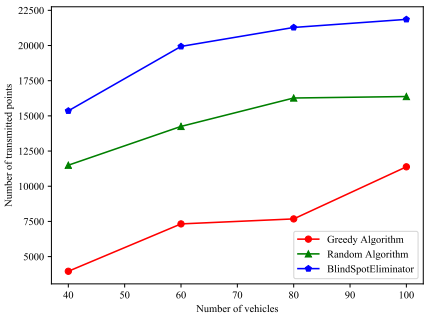

(d) Line graph of number of transmission points as vehicle quantity varies.

Fig. 2: Four comparison charts among three algorithms.

city roundabout scene with 80 vehicles in the CARLA simulator. As shown in figure 1, all vehicles in the scene are equipped with LiDAR and have V2X communication capabilities for collaborative perception. We collected point cloud data for all vehicles in this scenario and applied BlindSpotEliminator as well as two comparative methods on this data

Many factors determine the number of points to be transmitted, such as vehicle density, communication range, and resource block number. To reduce the randomness of single computations, we performed 15 calculations under the same conditions and calculated the number of transmitted points after each transmission. Figure 2(a) shows that BlindSpotEliminator outperforms the greedy algorithm and transmits 20% more point cloud data than the random algorithm under the best-case scenario. Secondly, we found that the number of transmitted points decreases with increased communication time slots. We believe this is due to the gradually decreasing number of communication blind spots available as time slots increase, leading to an increased likelihood of communication conflicts.

We conducted several comparative experiments to investigate the impact of the Cellular V2X communication range on the overall transmission point count. As shown in figure 2(b), we set up comparison experiments with communication ranges from 40 to 100 meters. After the experiments, we found that the number of transmitted points decreased as the communication distance increased. We speculate that this phenomenon occurs because the increase in communication distance significantly increases the likelihood of communication conflicts, thereby reducing the number of transmitted points.

Additionally, we conducted experiments to study the impact of resource block quantity on the number of transmitted points. As shown in figure 2(c), we set up comparative experiments with resource block quantities ranging from 15 to 55. We found that the number of transmitted points increased with an increase in resource block quantity, which is an expected result. However, due to the randomness of the random transmission method, there were occasional instances where an increase in resource block quantity decreased the number of transmitted points.

Finally, we conducted corresponding experiments to investigate the effect of the number of vehicles on the transmitted point cloud data. As shown in figure 2(d), we set up comparative experiments with vehicle numbers ranging from 40 to 100. After the experiment, we found that the transmitted point cloud data increases with the increase in the number of vehicles. However, it should be noted that for BlindSpotEliminator and the random algorithm, the rate of increase in transmitted point cloud data is gradually slowing down. We believe that the

reason for this phenomenon is that with the increase in vehicle density, there are more links, which leads to an increase in the overall transmitted point cloud data. However, too much vehicle density can lead to a higher probability of conflicts, which slows the rate of increase in transmitted point cloud data.

C. Qualitative Evaluation

In order to better illustrate the research significance of this paper, we designed a simplified specific scenario. As shown in figure 3(a), four vehicles, A, B, C, and D, can participate in collaborative perception at a roundabout intersection in a city (solid-line circles in the figure represent the vehicles, and the dashed-line areas represent blind spots). These four vehicles are all equipped with LiDAR and have the ability to share their point cloud data with other vehicles. Vehicle A is obstructed by two vehicles in front and to its right and cannot directly observe vehicles B and C. In addition, there are two blind spots, a and b, in its field of view. Furthermore, due to the obstruction of the central roundabout, vehicle A cannot observe the relevant information of vehicle D and blind spot c.

Similarly, figure 3(b) shows the BEV representation of the point cloud data for vehicles A, B, C, and D. The possible locations of the corresponding vehicles are indicated by solid-line boxes in the image. In the BEV representation of vehicle A, it is evident that there is no point cloud data observable in the blind spots a, b, and c, which are represented by blank areas in the image.

To enhance the effectiveness of collaborative perception, we employed the BlindSpotEliminator in this scenario. After five time slots of transmission, figure 3(c) shows the BEV representation of the point cloud data for vehicle A. To demonstrate the degree of communication resource conservation achieved by the BlindSpotEliminator, figure 3(d) shows the BEV representation of the overall fusion of the point cloud data for vehicles A, B, C, and D. In figure 3(c), it can be observed that vehicle A has acquired most of the point cloud data in the blind spots a, b and c. However, compared to figure 3(d), it has not acquired some unimportant information. Therefore, BlindSpotEliminator enables autonomous vehicles to obtain blind spot point cloud data while conserving communication resources, resulting in a better collaborative perception effect.

VI. Conclusion

BlindSpotEliminator considers various factors, including the distribution of vehicle blind spots and communication network conflict relationships. The aim is to maximize the utilization of communication resources, eliminate the number of blind spots, and improve the overall efficiency of collaborative perception in vehicular scenarios. Our method outperforms random and greedy algorithms, even in complex traffic scenarios. To further validate the reliability of BlindSpotEliminator, we conducted experiments using the Carla simulator, generating complex and specific traffic scenarios.

However, there are still areas for improvement in this paper. First, there is room for optimization in the modeling process. BlindSpotEliminator requires hundreds of seconds to calculate the optimal solution in large-scale traffic scenarios (referring to scenarios with hundreds of autonomous vehicles), which cannot meet the real-time requirements of collaborative perception. Pruning can be used to optimize the solution. Second, BlindSpotEliminator has not been tested on real-world data. Since this paper designs traffic scenarios and data using the CARLA simulator, it cannot fully represent the behavior of vehicles in real-world traffic scenarios. As data collection in the real world is time-consuming and expensive, paper [40], paper [41], and paper [42] suggests using neural networks to generate synthetic data, which is worth considering. Finally, one of the assumptions of this paper is that all vehicles are trustworthy, but in real-world scenarios, there are inevitably malicious devices and nodes. Paper [43] considers a graph-based learning approach to identify reliable vehicles in the network, and future improvements to BlindSpotEliminator should consider similar methods.

References

[1] T. Gao, H. Pan and H. Gao, "Monocular 3D Object Detection With Sequential Feature Association and Depth Hint Augmentation," in IEEE Transactions on Intelligent Vehicles, vol. 7, no. 2, pp. 240-250, June 2022, doi: 10.1109/TIV.2022.3143954.

[2] Pan X, Xia Z, Song S, et al. 3d object detection with pointformer[C]//Proceedings of the IEEE/CVF Conference on Computer Vision and Pattern Recognition. 2021: 7463-7472.

[3] Yang B, Luo W, Urtasun R. Pixor: Real-time 3d object detection from point clouds[C]//Proceedings of the IEEE conference on Computer Vision and Pattern Recognition. 2018: 7652-7660.

[4] K. Samal, H. Kumawat, P. Saha, M. Wolf and S. Mukhopadhyay, "Task-Driven RGB-Lidar Fusion for Object Tracking in Resource-Efficient Autonomous System," in IEEE Transactions on Intelligent Vehicles, vol. 7, no. 1, pp. 102-112, March 2022, doi: 10.1109/TIV.2021.3087664.

[5] Yang Q, Fu S, Wang H, et al. Machine-learning-enabled cooperative perception for connected autonomous vehicles: Challenges and opportunities[J]. IEEE Network, 2021, 35(3): 96-101.

[6] Liu Y C, Tian J, Ma C Y, et al. Who2com: Collaborative perception via learnable handshake communication[C]//2020 IEEE International Conference on Robotics and Automation (ICRA). IEEE, 2020: 6876-6883.

[7] Y. Tian, J. Wang, Y. Wang, C. Zhao, F. Yao and X. Wang, "Federated Vehicular Transformers and Their Federations: Privacy-Preserving Computing and Cooperation for Autonomous Driving," in IEEE Transactions on Intelligent Vehicles, vol. 7, no. 3, pp. 456-465, Sept. 2022, doi: 10.1109/TIV.2022.3197815.

[8] Marvasti E E, Raftari A, Marvasti A E, et al. Cooperative lidar object detection via feature sharing in deep networks[C]//2020 IEEE 92nd Vehicular Technology Conference (VTC2020-Fall). IEEE, 2020: 1-7.

[9] Cao D, Wang X, Li L, et al. Future directions of intelligent vehicles: Potentials, possibilities, and perspectives[J]. IEEE Transactions on Intelligent Vehicles, 2022, 7(1): 7-10.

[10] J. Li et al., "Learning for Vehicle-to-Vehicle Cooperative Perception Under Lossy Communication," in IEEE Transactions on Intelligent Vehicles, doi: 10.1109/TIV.2023.3260040.

[11] R. Molina-Masegosa and J. Gozalvez, "LTE-V for sidelink 5G V2X vehicular communications: A new 5G technology for shortrange vehicle-to-everything communications," IEEE Veh. Technol. Mag., vol. 12, no. 4, pp. 30–39, Dec. 2017.

[12] Q. Meng, H. Guo, J. Li, Q. Dai and J. Liu, "Vehicle Trajectory Prediction Method Driven by Raw Sensing Data for Intelligent Vehicles," in IEEE Transactions on Intelligent Vehicles, doi: 10.1109/TIV.2023.3265412.

[13] Gu B, Chen W, Alazab M, et al. Multiagent Reinforcement Learning-Based Semi-Persistent Scheduling Scheme in C-V2X Mode 4[J]. IEEE Transactions on Vehicular Technology, 2022, 71(11): 12044-12056.

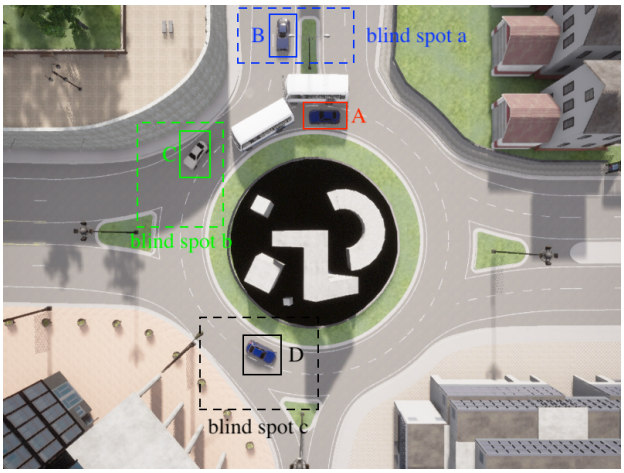

(a) The bird's-eye view photograph.

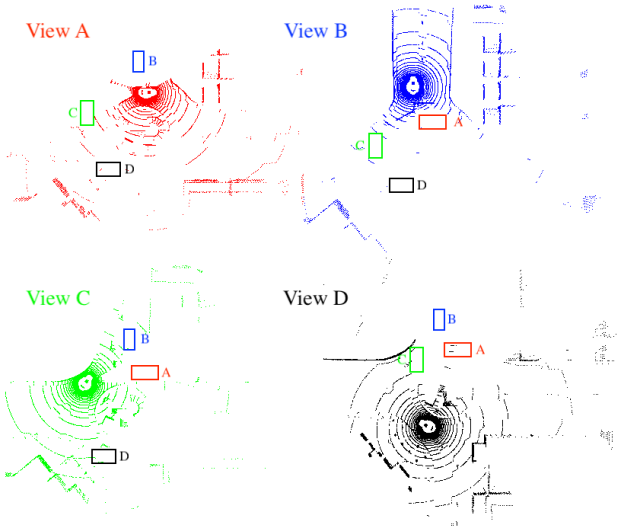

(b) The BEV graph of four vehicles.

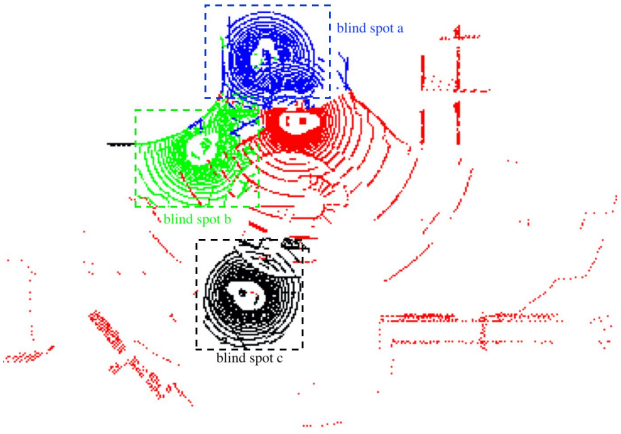

(c) BEV graph of all vehicles.

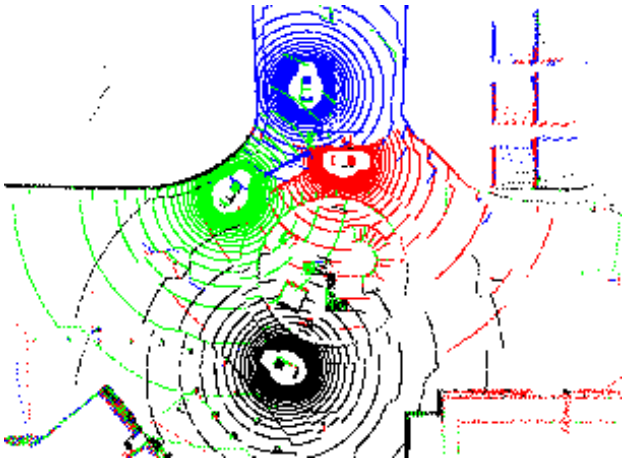

(d) Comparison of BEV graph.

Fig. 3: Four graphs for qualitative evaluation.

[14] Y. Hoshen, "VAIN: Attentional multi-agent predictive modeling," in Proc. 31st Int. Conf. Neural Inf. Process. Syst. (NIPS), Long Beach, CA, USA, 2017, pp. 2701–2711.

[15] Y.-C. Liu, J. Tian, N. Glaser, and Z. Kira, "When2com: Multi-agent perception via communication graph grouping," in Proc. IEEE/CVF Conf. Comput. Vis. Pattern Recognit. (CVPR), Seattle, WA, USA, 2020, pp. 4105–4114.

[16] W. Zhuang et al., "SDN/NFV-Empowered Future IoV with Enhanced Communication, Computing, and Caching," Proc. IEEE, vol. 108, no. 2, Feb. 2020, pp. 274–91.

[17] M. Li, P. Si, and Y. Zhang, "Delay-Tolerant Data Traffic to Software-Defined Vehicular Networks with Mobile Edge Computing in Smart City," IEEE Trans. Vehic. Tech., vol. 67, no. 10, Oct. 2018, pp. 9073–86.

[18] Y. He, N. Zhao, and H. Yin, "Integrated Networking, Caching, and Computing for Connected Vehicles: A Deep Reinforcement Learning Approach," IEEE Trans. Vehic. Tech., vol. 67, no. 1, Jan. 2018, pp. 44–55.

[19] Z. Zhu, N. Pivaro, S. Gupta, A. Gupta and M. Canova, "Safe Model-Based Off-Policy Reinforcement Learning for Eco-Driving in Connected and Automated Hybrid Electric Vehicles," in IEEE Transactions on Intelligent Vehicles, vol. 7, no. 2, pp. 387-398, June 2022, doi: 10.1109/TIV.2022.3150668.

[20] C. Shu and Y. Luo, "Multi-Modal Feature Constraint based Tightly Coupled Monocular Visual-LiDAR Odometry and Mapping," in IEEE Transactions on Intelligent Vehicles, 2022, doi: 10.1109/TIV.2022.3215141. 202

[21] Sandhya P, Azad A P, Kim Y, et al. Augmented conflict-free Scheduling for low power WSNs[C]//2015 12th Annual IEEE Consumer Communications and Networking Conference (CCNC). IEEE, 2015: 425-430.

[22] Chen C, Xu Q, Cai M, et al. Conflict-free cooperation method for connected and automated vehicles at unsignalized intersections: Graph-based modeling and optimality analysis[J]. IEEE Transactions on Intelligent Transportation Systems, 2022, 23(11): 21897-21914.

[23] Zhan C, Gao K. Conflict-free scheduling for partially connected D2D networks with network coding[J]. IEEE Wireless Communications Letters, 2016, 5(5): 456-459.

[24] Naghsh Z, Valaee S. Conflict-Free Scheduling in Cellular V2X Communications[J]. IEEE/ACM Transactions on Networking, 2020, 29(1): 106-119.

[25] Naghsh Z, Valaee S. Delay-aware conflict-free scheduling for LTE-V, sidelink 5G V2X vehicular communication, in highways[C]//2018 52nd Asilomar Conference on Signals, Systems, and Computers. IEEE, 2018: 1452-1456.

[26] J. Su, Z. Liu, Y. -a. Xie, K. Y. Chan and X. Guan, "Dynamic

Resource Allocation in Queue-Constrained and Delay-Sensitive Vehicular Networks," in IEEE Transactions on Intelligent Vehicles, doi: 10.1109/TIV.2023.3270269.
[27] Boutebel A, Atmani M, Boukredera D, et al. Multi-channel Conflict-Free Scheduling Algorithm for IEEE 802.15. 4e/TSCH Networks[C]//2022 International Conference on Electrical, Computer and Energy Technologies (ICECET). IEEE, 2022: 1-6.
[28] Naghsh Z, Valaee S. MUCS: A new multichannel conflict-free link scheduler for cellular V2X systems[C]//2018 IEEE International Conference on Communications (ICC). IEEE, 2018: 1-7.
[29] Cheng M, Ye Q. Transmission scheduling based on a new conflict graph model for multicast in multihop wireless networks[C]//2012 IEEE Global Communications Conference (GLOBECOM). IEEE, 2012: 5717-5722.
[30] Li X, Shankaran R, Orgun M, et al. Joint autonomous resource selection and scheduled resource allocation for D2D-based V2X communication[C]//2018 IEEE 87th Vehicular Technology Conference (VTC Spring). IEEE, 2018: 1-5.
[31] P. Lang, D. Tian, X. Duan, J. Zhou, Z. Sheng and V. C. M. Leung, "Cooperative Computation Offloading in Blockchain-Based Vehicular Edge Computing Networks," in IEEE Transactions on Intelligent Vehicles, vol. 7, no. 3, pp. 783-798, Sept. 2022, doi: 10.1109/TIV.2022.3190308.
[32] M. Roth, J. Stapel, R. Happee and D. M. Gavrila, "Driver and Pedestrian Mutual Awareness for Path Prediction and Collision Risk Estimation," in IEEE Transactions on Intelligent Vehicles, vol. 7, no. 4, pp. 896-907, Dec. 2022, doi: 10.1109/TIV.2021.3138944.
[33] A. Muraleedharan, H. Okuda and T. Suzuki, "Real-Time Implementation of Randomized Model Predictive Control for Autonomous Driving," in IEEE Transactions on Intelligent Vehicles, vol. 7, no. 1, pp. 11-20, March 2022, doi: 10.1109/TIV.2021.3062730.
[34] X. Zhu et al., "Interaction-Aware Cut-In Trajectory Prediction and Risk Assessment in Mixed Traffic," in IEEE/CAA Journal of Automatica Sinica, vol. 9, no. 10, pp. 1752-1762, October 2022, doi: 10.1109/JAS.2022.105866.
[35] R. Singh, D. Saluja and S. Kumar, "R-Comm: A Traffic Based Approach for Joint Vehicular Radar-Communication," in IEEE Transactions on Intelligent Vehicles, vol. 7, no. 1, pp. 83-92, March 2022, doi: 10.1109/TIV.2021.3074389.
[36] D. Maturana and S. Scherer, "Voxnet: A 3d convolutional neural network for real-time object recognition," in 2015 IEEE/RSJ International Conference on Intelligent Robots and Systems (IROS). IEEE, 2015, pp.922–928.
[37] Y. Zhou and O. Tuzel, "Voxelnet: End-to-end learning for point cloud based 3d object detection," in Proceedings of the IEEE conference on computer vision and pattern recognition, 2018, pp. 4490–4499.
[38] A. H. Lang, S. Vora, H. Caesar, L. Zhou, J. Yang, and O. Beijbom, "Pointpillars: Fast encoders for object detection from point clouds," in 2019 IEEE/CVF Conference on Computer Vision and Pattern Recognition (CVPR), 2019, pp. 12 689–12 697.
[39] T. -H. Chen and T. S. Chang, "RangeSeg: Range-Aware Real Time Segmentation of 3D LiDAR Point Clouds," in IEEE Transactions on Intelligent Vehicles, vol. 7, no. 1, pp. 93-101, March 2022, doi: 10.1109/TIV.2021.3085827.
[40] S. Huch, L. Scalerandi, E. Rivera and M. Lienkamp, "Quantifying the LiDAR Sim-to-Real Domain Shift: A Detailed Investigation Using Object Detectors and Analyzing Point Clouds at Target-Level," in IEEE Transactions on Intelligent Vehicles, doi: 10.1109/TIV.2023.3251650.
[41] X. Li, H. Duan, Y. Tian and F. -Y. Wang, "Exploring Image Generation for UAV Change Detection," in IEEE/CAA Journal of Automatica Sinica, vol. 9, no. 6, pp. 1061-1072, June 2022, doi: 10.1109/JAS.2022.105629.
[42] L. Yang et al., "Collective Entity Alignment for Knowledge Fusion of Power Grid Dispatching Knowledge Graphs," in IEEE/CAA Journal of Automatica Sinica, vol. 9, no. 11, pp. 1990-2004, November 2022, doi: 10.1109/JAS.2022.105947.
[43] B. B. Gupta, A. Gaurav, E. C. Marín and W. Alhalabi, "Novel Graph-Based Machine Learning Technique to Secure Smart Vehicles in Intelligent Transportation Systems," in IEEE Transactions on Intelligent Transportation Systems, doi: 10.1109/TITS.2022.3174333.